Chapter

Unique Surface Modifications on Diamond Thin Films

Vadali Venkata Satya Siva Srikanth

Abstract

Diamond thin films are touted to be excellent in surface-sensitive sensing, electro-mechanical systems, and electrochemical applications. However, these applications often entail patterned active surfaces and subtle chemical surface modifications. But due to diamond's intrinsic hardness and chemical inertness, surface patterning (using micro-machining and ion etching) and chemical surface modifications, respectively, are very difficult. In the case of surface patterning, it is even more challenging to obtain patterns during synthesis. In this chapter, the direct patterning of sub-wavelength features on diamond thin film surface using a femto-second laser, rapid thermal annealing as a means to prepare the diamond thin film surface as an efficient direct charge transfer SERS substrate (in metal/insulator/semiconductor (MIS) configuration), and implantation of $^{14}N^{+}$ ions into the surface and sub-surface regions for enhancing the electrical conductivity of diamond thin film to a certain depth (in MIS configuration) will be discussed encompassing the processing strategies and different post-processing characteristics.

Keywords: diamond, thin films, surface patterning, rapid thermal annealing, ion implantation

1. Introduction

Scientists working on diamonds realized long back that the unsurpassed properties of a diamond could be tapped for many applications only when synthesized in thin-film form. Since then, chemical vapor deposition (CVD) [1, 2] has been the most generally used technique to synthesize various diamond thin films for multiple applications. CVD of diamond involves the low-pressure growth of a thin film of a network of tetrahedrally bonded carbon atoms (on a diamond-seeds pre-treated substrate) from a suitable gas phase. CVD of diamond thin films typically involves activation of the appropriate gas mixtures (for example, a mixture of H_2 and CH_4 under low pressure activated by microwave energy), gas-phase reactions (leading to the formation of diamond forming gas species), diffusion of the diamond forming gas species onto the substrate and formation of a non-volatile thin layer of tetrahedrally bonded carbon atoms network. By controlling the CVD process parameters (namely substrate pre-treatment, substrate temperature, reaction pressure, and gas mixture composition), diamond thin films with a variety of grains, namely epitaxial, highly oriented, polycrystalline, and nanocrystalline grains, can be obtained. When diamond forming gas species reach the substrate's surface, adhere to it, and settle quickly into possible equilibrium positions before any structural defects form on the thin film growth front, a single crystalline

diamond thin film is obtained. On the contrary, when the diamond forming gas species do not quickly settle into stable equilibrium positions upon their arrival at the substrate's surface, nanocrystalline diamond film is obtained.

With the extraordinary and diverse properties that diamond thin films possess, they have a wide range of application potential [3, 4]. However, to realize the complete application potential of diamond thin films, their surface modification is inevitable, especially in surface-sensitive sensing, electro-mechanical systems, and electrochemical applications. Any surface modification process typically modifies a selected diamond thin film's surface by bringing physical, chemical, or biological characteristics different from those found on the surface of the as-deposited diamond film. Methods such as plasma and ion etching, colloidal crystal templating method, selective area CVD, molding, traditional lithography are available to obtain patterned diamond surfaces. Single crystal, as well as polycrystalline diamond surfaces, were exploited to fabricate cantilevers, whiskers, tips, and gratings.

In this chapter, unique surface modifications, namely the direct patterning of sub-wavelength features on the surface of a diamond thin film using a femtosecond laser [5, 6], rapid thermal annealing (RTA) as a means to prepare the surface of a diamond thin film as an efficient direct charge transfer surface-enhanced Raman scattering (SERS) substrate [5, 7], and implantation of $^{14}N^{+}$ ions into the surface and sub-surface regions of a diamond thin film to enhance its surface electrical conductivity [8] will be discussed. The surface of a typical polycrystalline diamond thin film (deposited on Si substrate using CVD) will be considered as the surface to be modified. The discussion will encompass the modification method and post-modification characteristics of modified diamond thin films.

2. Direct surface patterning using femtosecond laser

Irradiation with a femtosecond (fs) laser beam has been touted as a better technique for surface patterning (through ablation) of ultra-hard materials. In this context, the single-crystal diamond surface has been micromachined or patterned by irradiating the surface with high-energy fs-laser pulses. Surfaces of polycrystalline diamond thin films have also been patterned using fs-laser irradiation. In this section, direct surface patterning on polycrystalline diamond thin film using polarization-controlled surface plasmon (SP)-fs laser coupling mechanism will be explained [5, 6]. The polycrystalline diamond film considered here was grown on Si (100) substrate using microwave plasma-enhanced CVD for 6 h at a substrate temperature of 700°C and gas pressure of 25 Torr. Less than 1% of methane (CH_4) in hydrogen (H_2) was used as the reaction gas mixture. Before the thin film deposition, the Si substrate was scratched manually against a thick quartz plate with a synthetic polycrystalline diamond paste (~1 μm) in between. After diamond seeding, the residue was removed by ultrasonically cleaning the substrate with acetone, followed by cleaning with ethanol, then dried in air at room temperature.

The schematic of the experimental setup used for the direct fs-laser patterning on the diamond thin film surface under ambient conditions is shown in **Figure 1**. Ti:Sapphire oscillator-amplifier system operating at a wavelength (λ) of ~800 nm and delivering 110 fs, 1 mJ output energy pulses at a repetition rate of 1 kHz was used to irradiate the considered diamond thin film surface. The fs-laser pulses are linearly polarized. The laser pulse energy was adjusted to 200–500 nJ using neutral density (ND) filters and a combination of half-wave plate and polarizer. The laser beam was focused onto the diamond thin film surface using an objective with a numerical aperture of 0.4, and patterning was performed transversely to the laser propagation direction. The laser spot size on the surface was ~2.4 μm.

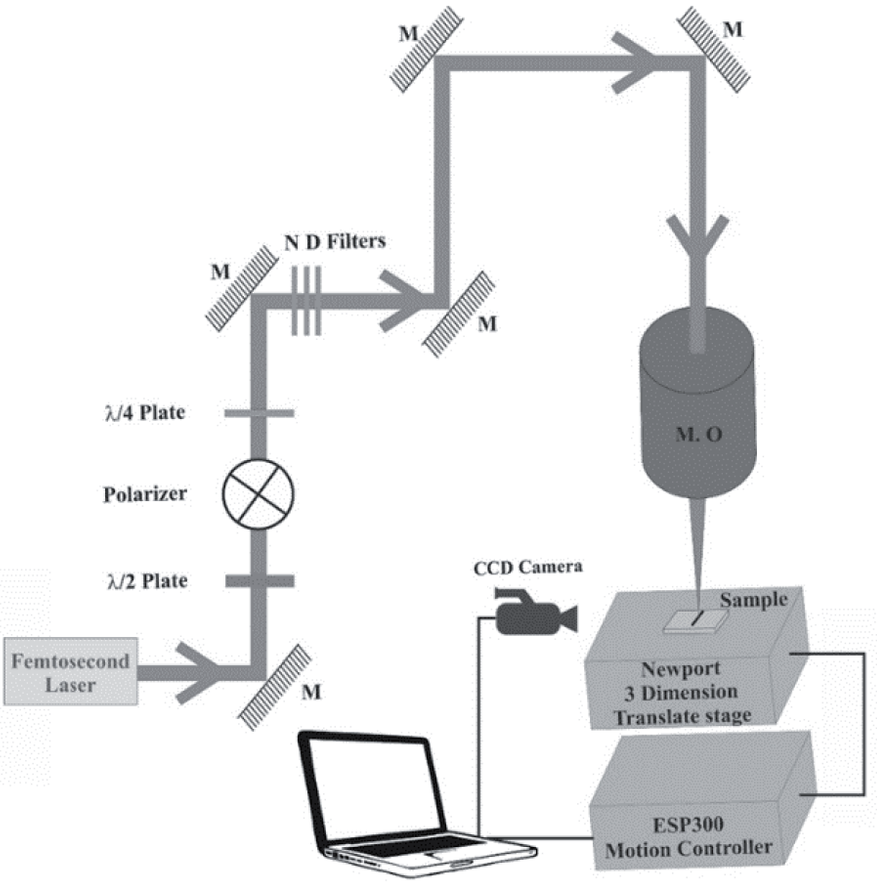

Figure 1.
Schematic of fs-laser direct writing experimental setup [5].

Computer-controlled translational stages were used to translate the sample in x, y, and z directions. A CCD camera with high magnification was used to control the sample surface's focal depth and monitor the patterning process. Transverse patterning geometry (in which the stage is translated perpendicular to the laser beam propagation direction) was used to pattern the surface. Transverse patterning geometry was preferred over longitudinal patterning geometry because it provides much greater flexibility and allows to write patterned structures of arbitrary length.

Plane-view scanning electron micrographs of the as-deposited and fs-laser irradiated diamond thin film surfaces are shown in **Figure 2(a)–(h)**. The surface of the as-deposited thin film (**Figure 2(a)**) is constituted by polycrystalline diamond grains. **Figure 2(b)–(d)** show the low and high magnification plane-view SE micrographs of periodic features induced on the thin film surface with linearly polarized fs laser pulses having a pulse energy 380 nJ. An overview of the fs-laser irradiated region is shown in **Figure 2(b)**. Depending on the laser polarization, morphological and topographical changes are observed in the central area of the irradiated region. Irrespective of the scanning direction, linear periodic ripples perpendicular to the laser polarization and nearly circular ripple features are induced due to linear and circularly polarized light irradiation, respectively. The energy threshold for generating periodic surface features is 200 nJ in the present case. The energy threshold may vary depending on the quality of the diamond thin film considered for surface patterning. The laser-induced periodic surface features have a periodicity of ~180 nm (4.4 times < the free-space λ of the laser and 1.85 times < the λ of the laser in diamond). The width of the fringes is ~80 nm, and the orientations of the fringes are perpendicular to the laser polarization.

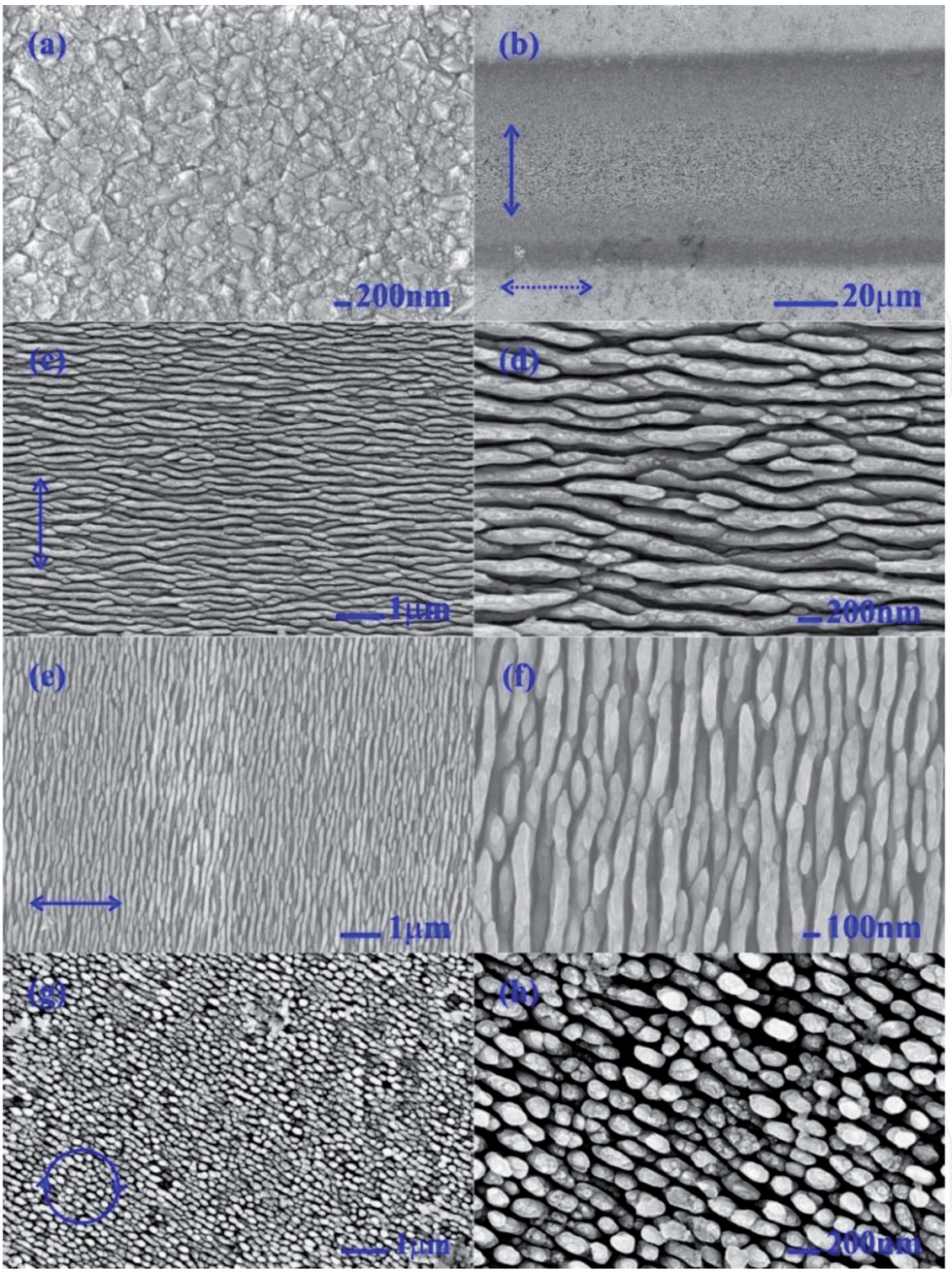

Figure 2.
Plane-view scanning electron micrographs of as-deposited and fs-laser irradiated polycrystalline diamond thin film surface under different experimental conditions: (a) morphology of as-deposited film; (b), (c), (d), (e), and (f) periodic surface features (ripples) obtained using linearly polarized laser pulses having a pulse energy of 380 nJ; (g) and (h) near-circular surface features obtained using circularly polarized laser pulses having a pulse energy of 410 nJ. The polarization and the scanning directions are indicated by the solid and dotted arrows, respectively. In all the above cases, the film surface was moved at ~100 μm/sec w.r.t. to the irradiating fs-laser. (Reprinted with permission from Kuntumalla et al. [6]).

Similar results obtained in parallel and perpendicular scanning (w.r.t. laser polarization) unambiguously show that the scanning direction does not influence the morphology and orientation of the surface features. If the laser polarization direction is flipped by 90° using a half-wave plate in the optical path, the direction of the periodic surface features also flipped by 90°, as shown in **Figure 2(e)** and **(f)**.

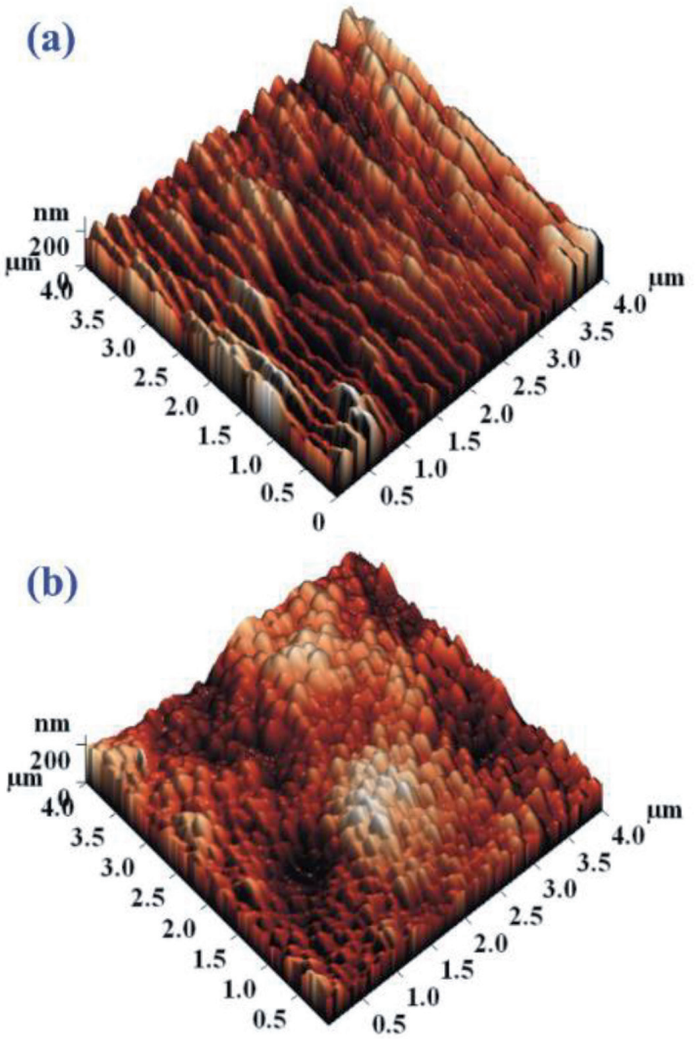

Figure 3.
Surface topography (obtained using atomic force microscopy) of fs-laser irradiated diamond thin film surfaces. (a) Represents features obtained using linear polarized light, while (b) represents features obtained using circularly polarized light. (Reprinted with permission from Kuntumalla et al. [6]).

Irradiation of the thin film surface with circularly polarized fs-laser resulted in nearly circular surface features with lateral sizes in the range ~ 100–200 nm, as shown in **Figure 2(g)** and **(h)**. Raman scattering analysis showed that the fs-laser irradiation had only caused minimal graphitization on the patterned diamond film surface [6]. Similarly, X-ray diffraction analysis showed the crystallinity of the patterned surface was intact. RMS roughness values of laser irradiated surfaces constituting linear (**Figure 3(a)**) and circular (**Figure 2(b)**) surface features were in the range 42–46 nm. This acceptable increase in RMS roughness from the original value of ~30 nm is an important characteristic that is often looked for during surface fabrication methods like the one presented here.

Here, the spatial period (Λ) of the surface ripples formed by the interference of laser with surface plasmons (SPs) is expressed as Eq. (1)

$$\Lambda = \frac{\lambda}{\frac{\lambda}{\lambda_s} \pm sin\theta} \tag{1}$$

where λ and λ_s are the wavelengths of incident laser and SPs, respectively. θ is the incident angle of the fs-laser. λ_s can be obtained from the dispersion Eq. (2)

$$\lambda_s = \lambda\left(\frac{\varepsilon' + \varepsilon_d}{\varepsilon'\varepsilon_d}\right)^{1/2} \quad (2)$$

for metal/dielectric interface. Here, ε′ is the imaginary part of permittivity, and ε_d is the dielectric constant of the dielectric material (here air since the experiments are carried out in ambient conditions). Here, the laser is incident normally (i.e., θ = 0°) on the diamond thin film surface and the dielectric constant of air is 1(i.e., ε_d = 1). Therefore, the period can be expressed as Eq. (3)

$$\Lambda = \lambda_s = \lambda\left(1 + \frac{1}{\varepsilon'}\right) \quad (3)$$

Eqs. (1)–(3) are considered here because it is widely accepted that a semiconductor or dielectric (or even metallic) surface such as the diamond thin film surface, when irradiated by ultrashort pulse laser such as fs-laser with damage threshold fluence, will be under highly excited state and behaves like metal surface. When irradiated with fs-laser pulse energy in the range 200–500 nJ, the diamond surface here acts like a metallic liquid carbon fulfilling the metallic state condition, i.e., ε′ < −1. In this state, the formation of SPs is facilitated. Once SPs are formed, they undergo interference with the laser light leading to the formation of deep-subwavelength ripples (Λ/λ = ~0.22 as experimentally obtained). As the thin film surface is translated, the already formed periodicity favors nonlinear absorption of laser energy at an identical spatial distribution, allowing the periodicity to be maintained. The formation of near-circular periodic surface features (as shown in **Figure 2(g)** and **(h)**) is plausibly due to the axisymmetric distribution of the electric field vector of the circularly polarized laser.

3. RTA to prepare direct charge transfer SERS surface

Surface-enhanced Raman scattering (SERS) based analytical bio-sensing requires stable, durable, and reusable SERS active surfaces. However, the typical SERS surfaces do not have long-term stability, mainly owing to the instability of metal nanostructures deposited on SERS surfaces or due to the intrinsic nature of the SERS surfaces themselves. In this context, a modified diamond thin film surface can be touted as an excellent SERS surface owing to its inherent properties, namely electronic and mechanical properties, chemical stability/inertness, and biocompatibility. Typically SERS activity of diamond surfaces is achieved by depositing suitable metal nanoclusters on their surfaces. The SERS activity in such cases is explained in terms of the electromagnetic enhancement mechanism [5, 7]. In the electromagnetic enhancement mechanism, there is a charge transfer from the Fermi level of the metal nanoclusters to the lowest unoccupied molecular orbital (LUMO) of the adsorbed analyte molecules on the SERS surface. The charge transfer changes the effective polarizability of the adsorbed analyte molecules, resulting in the observed SERS activity.

In this section, the diamond thin film surface modified using rapid thermal annealing (RTA) (i.e., without any metal nanostructures on the diamond thin film surface) will be elucidated as a direct charge transfer resonance-based SERS surface [7]. The diamond thin film considered in the previous section is also considered here for elucidation. The diamond thin film surface was rapidly thermal annealed at 1000°C (heating rate is 40°C/sec, soaking time is 30 sec, and cooling time is 5 min to reach room temperature) under N_2 atmosphere. The heating chamber used for

RTA is shown in **Figure 4**. The chamber consists of a quartz window with halogen lamps as infrared heat sources. The diamond thin film (with its surface facing the halogen lamps) was placed on the bedplate, fixed on an aluminum base plate. Since the heating source was on the top of the film's surface, any changes would start at the diamond thin film surface.

RTA changed the diamond film surface morphology from having sharp features with defined boundaries (**Figure 2(a)**) to a sponge-like surface without any well-defined boundaries. The cross-sectional scanning electron micrograph (**Figure 5**) shows that the sponge-like feature is 100 nm thick, and there is no change in the diamond morphology below the sponge-like layer. **Figure 6(a)** shows a plane-view scanning electron micrograph of the diamond film surface after RTA. It can be observed from **Figure 6(a)** that the annealed diamond film surface has an interconnected wire-like surface morphology, which is entirely different from the original morphology.

Further modifications were not made to the thermally annealed diamond thin film surface (test surface) before testing its SERS activity. Rhodamine6G (R6G) fluorescent dye molecules were used as the probe to understand the SERS activity. R6G molecules exhibit a large Raman scattering cross-section and have been used as probe molecules in SERS-based bio-sensing studies. 10 ml of $5x10^{-5}$ M Rhodamine (R) 6G aqueous solution was dropped onto the test surface and was allowed to

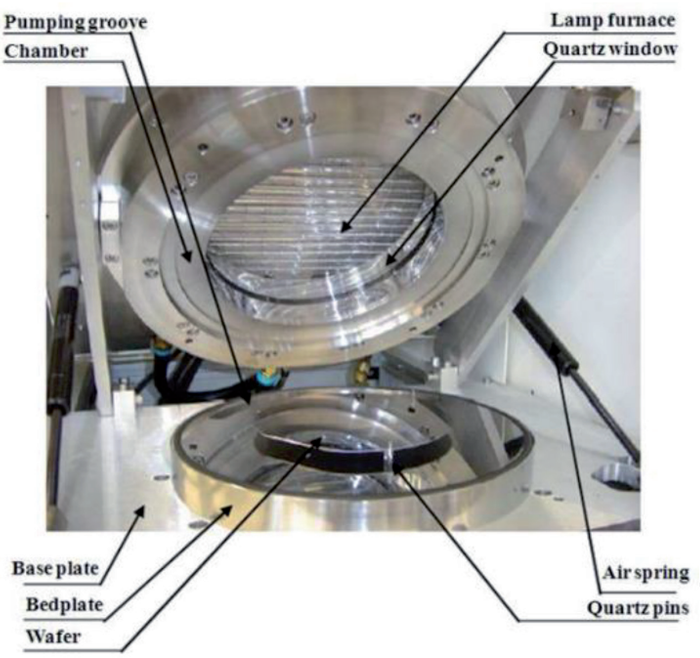

Figure 4.
Rapid thermal annealing chamber [5].

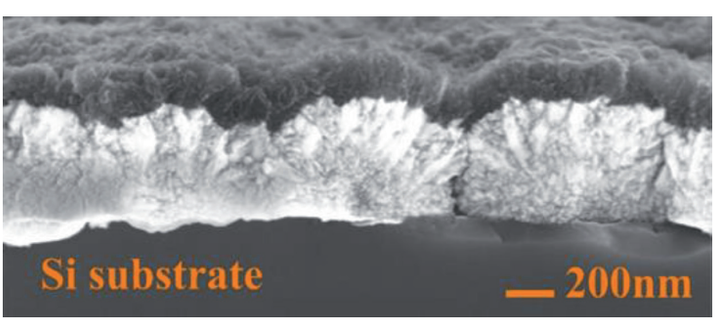

Figure 5.
Cross-sectional view scanning electron micrograph of thermally annealed diamond thin film shown in ***Figure 2(a)*** *[5].*

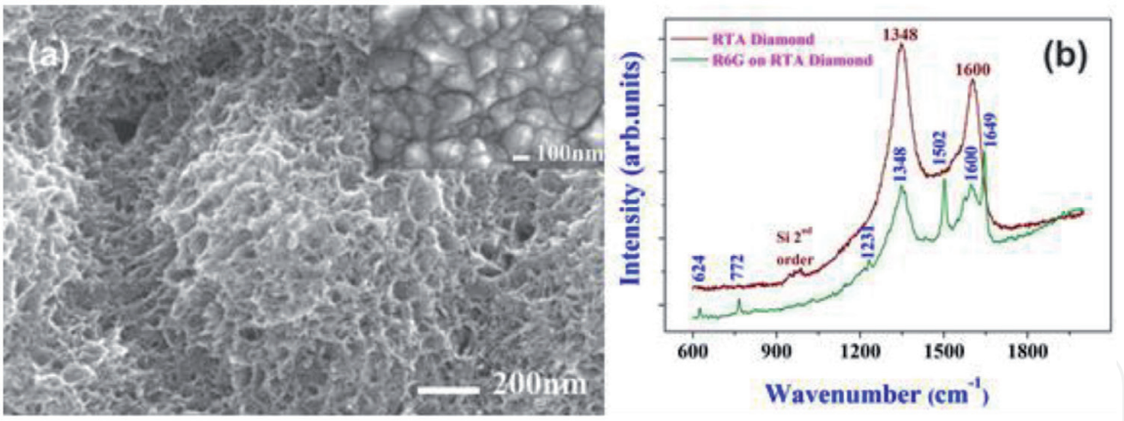

Figure 6.
(a) High magnification plane-view scanning electron micrograph of the thermally annealed diamond thin film surface. Inset: Morphology of as-deposited diamond film (b) Raman spectra obtained from the test surface and R6G ($5x10^{-5}$ M) adsorbed on the test surface. (Reprinted with permission from Kuntumalla et al. [7]).

dry naturally. Room temperature SERS activity of R6G molecules adsorbed on the test surface was recorded using a 514.5 nm laser. When R6G molecules are excited with a visible laser, they show molecular resonance Raman scattering in addition to the SERS effect that comes from the surface plasmon excitation. SERS signals are collected in backscattering geometry in the spectral range 50–2000 cm^{-1} with a spectral resolution of 1 cm^{-1}. **Figure 6(b)** shows Raman spectra obtained from the test surface and R6G adsorbed on the test surface. The Raman spectrum of the test surface shows two broad bands at 1348 and 1600 cm^{-1} correspond to polycrystalline- and nanocrystalline- graphite, respectively. The observation of graphite Raman bands confirms phase change from diamond to graphite due to RTA. SERS spectrum of R6G adsorbed on the test surface shows bands at 624, 772, 1502, and 1649 cm^{-1} corresponding to R6G in addition to the above-mentioned graphite bands.

The observation of strong SERS bands corresponding to very low concentration R6G molecules is a consequence of the charge transfer resonance process because there is no involvement of metal nanoclusters. It is important to note that Raman bands could not be detected when the same concentration of R6G molecules was adsorbed directly on the as-deposited diamond thin film surface. In the case of the as-deposited diamond thin film surface, the energy gap between the Fermi level of diamond surface (111) (−4.97 eV) (or − 5.3 eV for (100) surface) and the LUMO (−3.40 eV) of R6G molecule is about 1.57 eV (or 1.9 eV), which is closer to 2.41 eV, the energy of the incident laser. Hence signal enhancement should take place through the charge transfer resonance process. However, the as-deposited diamond thin film surface did not show SERS activity. In other words, even though the energy of the incident laser is higher than that of the energy gap between the Fermi level of diamond and LUMO of R6G, there is no charge transfer from diamond surface states to R6G molecule. In diamond, the carbon atoms are bonded in sp^3 hybridization (σ-bond). The heavily lopsided configuration of the sp^3 orbital allows a substantial overlap and a strong covalent bond (bonding electrons are tightly bound to the nuclei of the bonding carbon atoms) when the atom combines with the sp^3 orbital of another carbon atom. The thermally annealed diamond thin film surface is constituted by substantial amounts of graphitic-like sp^2 bonded carbon. In sp^2 bonded structure, three of four valence electrons of carbon are covalently bonded (σ-bond) while the fourth is free. Such delocalized electrons participate in π-bond formation between carbon atoms and can traverse between them. In the thermally annealed diamond thin film surface, the amount of sp^2 bonded carbon is considerably larger when compared with the as-deposited diamond thin film

surface. Therefore, in the thermally annealed diamond thin film, an enormous number of delocalized electrons are available to interact with the R6G molecule when the laser falls on R6G adsorbed test surface. This results in SERS activity thermally annealed diamond thin film. To further confirm, a typical diamond-like carbon (DLC) thin film surface was also tested (in similar lines to the thermally annealed diamond thin film surface), owing to its constitution by a considerable amount of sp^2 bonded carbon. DLC thin film also showed excellent SERS activity, proving that the thermally annealed diamond thin film surface is an excellent direct charge transfer resonance SERS surface. Additionally, due to the Metal (100 nm of a graphitic layer)-Insulator (diamond)-Semiconductor (Si substrate) (MIS) structure (**Figure 5**), it is easier to develop bio-sensing devices.

4. $^{14}N^+$ ions implantation to prepare an electrically conductive surface

Polycrystalline diamond thin films deposited on doped Si substrates can be made suitable for the fabrication of robust MIS type devices when the near-surface regions are made electrically conductivity. In addition to the RTA presented in the previous section, implantation of N^+ ions into the surface and sub-surface regions of a typical polycrystalline diamond thin film can be another way of achieving MIS structure. The polycrystalline diamond thin film (named F1) used in the previous two sections is again considered for the implantation of N^+ ions. The diamond thin film surface is implanted with 100 keV $^{14}N^+$ ions with fluences of 1E16 and 1E17 ions/cm^2 (the samples are referred to as F2 and F3, respectively). Implantation experiments are carried out at room temperature by maintaining a constant beam current of 10 μA under pressure < 10^{-7} mbar.

XRD patterns of as-deposited and N^+ ions' implanted diamond thin films are shown in **Figure 7**. The reflections corresponding to (111), (220), and (400) crystal planes in diamond are observed at 2θ = ~45.9, ~75.2, and ~ 91.4°, respectively, in all the samples implying that the crystallinity of the diamond thin films after implantation is intact. Moreover, no other reflections corresponding to any different crystalline phase were observed post-implantation, suggesting that the implantation did not convert diamond into any new phase. The diffraction peak broadening post-implantation is negligible, indicating that the implantation has not affected the

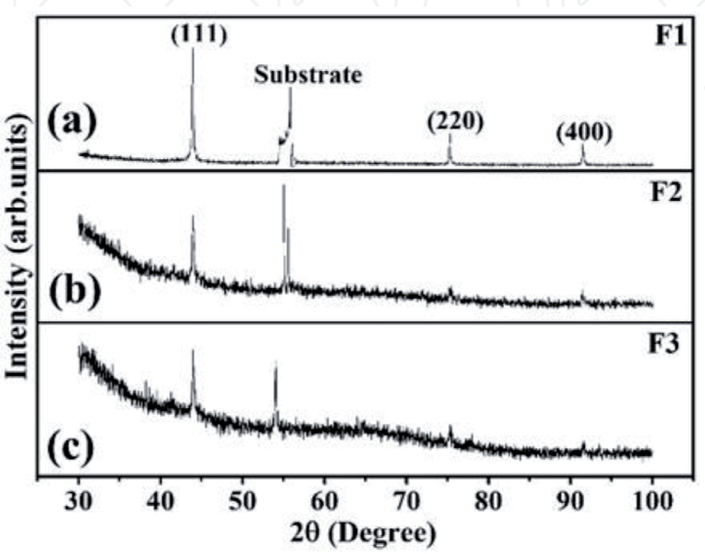

Figure 7.
X-ray diffractograms of (a) F1, (b) F2 and (c) F3. (Reprinted with permission from Bommidi et al. [8]).

grain size in the diamond films. **Figure 8** shows the plane-view scanning electron micrographs, which depict the typical randomly oriented diamond grains of F1 and N^+ ions' implanted diamond films (F2 and F3). However, in the case of F2 and F3, the grain edges appeared to be rounded-off most plausibly due to the selective sputtering effect of the N^+ ion beam on the grain boundary regions, which are primarily graphitic (sp^2 carbon) in nature.

To further understand the phase stability of diamond and the presence of any other phases in small quantities, the Raman spectra of all the samples are recorded and shown in **Figure 9**. F1 exhibited the characteristic zone center phonon in diamond at ~1333 cm^{-1} and graphitic band (G band, stretching mode of planar sp^2 C at the grain boundaries) at ~1500 cm^{-1}, which are typical for diamond films. The spectra of F2 and F3 indicated a change in the bonding environment in the implanted films. The peak fitted spectra are shown in **Figure 9(d–f)**. It is observed that the position, relative intensity, and bandwidth of diamond band, D band (1350 cm^{-1}, breathing mode of planar sp^2 C at the grain boundaries), and G band are different in F1, F2, and F3, indicating differences in phase content in these samples. Diamond, and D and G Raman bands in the case of F2 and F3 are slightly red-shifted compared to that in F1, indicating that implantation has induced in-plane tensile stresses and formation of sp^2 clusters and amorphous carbon in the diamond grain boundaries, respectively. Rutherford backscattering spectra (**Figure 10**) of all the samples are recorded to understand implantation depth. In F2 and F3, both C and N peaks are observed in the corresponding spectra. The width of N peak is ~75 nm which is close to the calculated (Stopping and Range of Ions in Matter (SRIM) software-based) depth of 88 nm for N atoms in diamond.

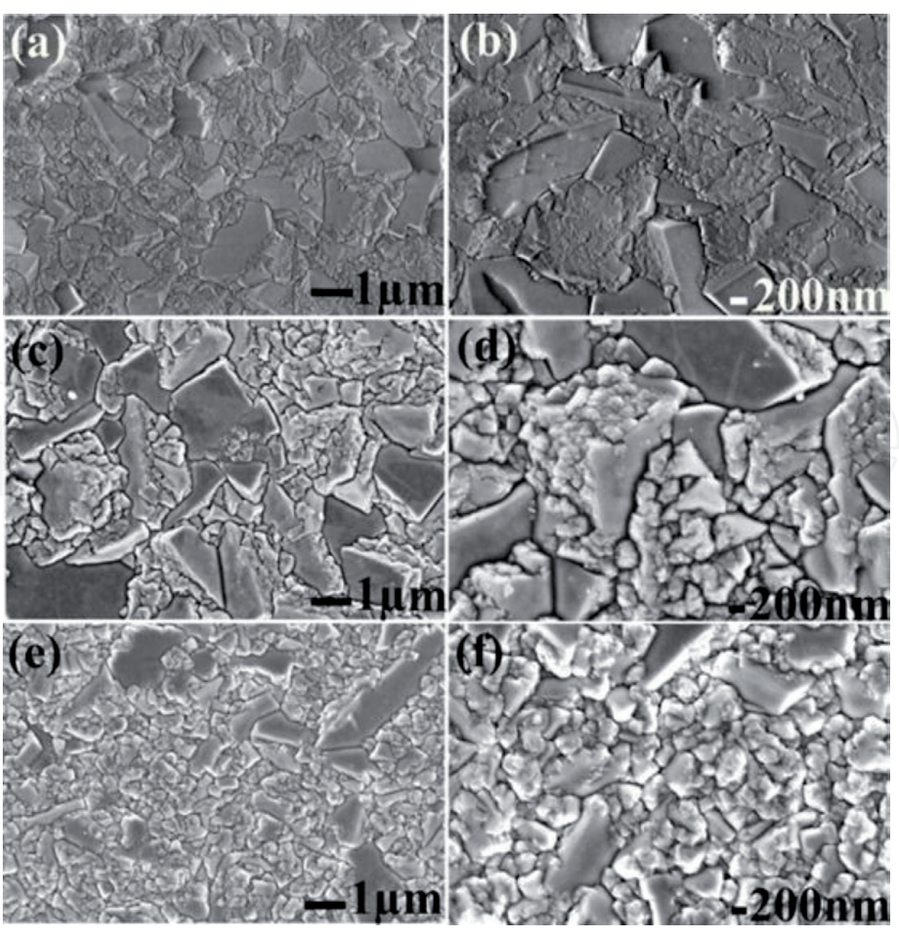

Figure 8.
Plane-view scanning electron micrographs (at different magnifications) of (a & b) F1, (c & d) F2 and (e & f) F3. (Reprinted with permission from Bommidi et al. [8]).

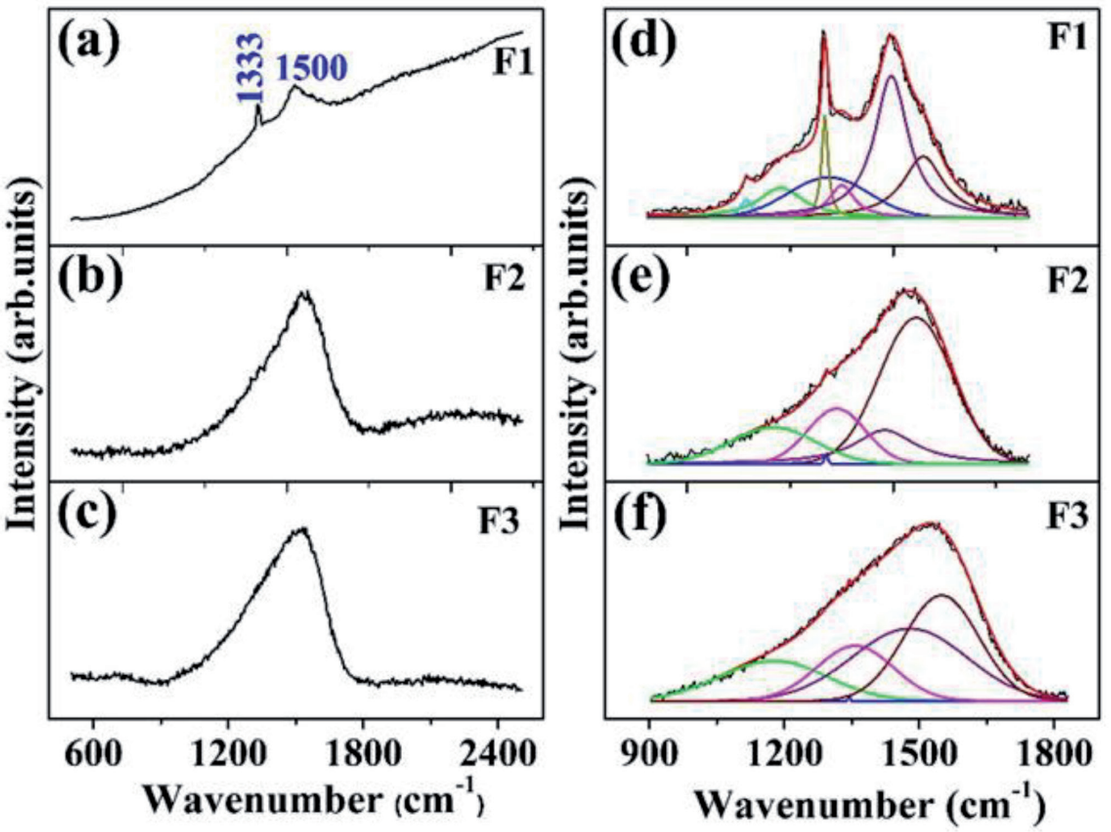

Figure 9.
Raman spectra of (a) F1, (b) F2 and (c) F3 and the corresponding best fitted spectra in (d), (e) and (f), respectively. (Reprinted with permission from Bommidi et al. [8]).

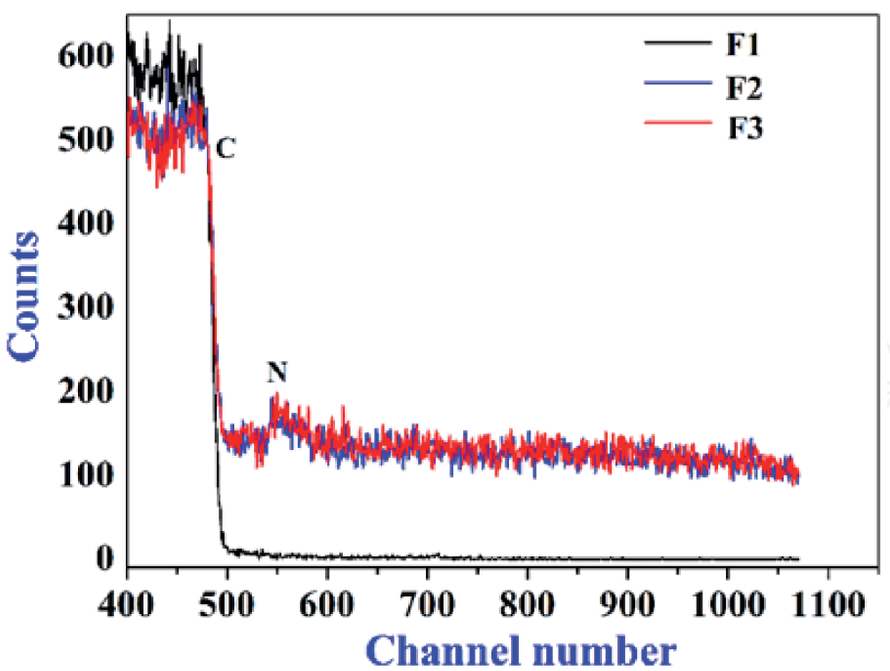

Figure 10.
Rutherford backscattering spectra of F2 and F3 in comparison to F1. (Reprinted with permission from Bommidi et al. [8]).

A local thermal spike (local temperature rise to a great degree) might have taken place in ion-irradiated diamond films [9]. As a consequence, graphitic content might have formed in F2 and F3. The combined effect of induced graphitization along the diamond grain boundaries and N atom incorporation is expected to

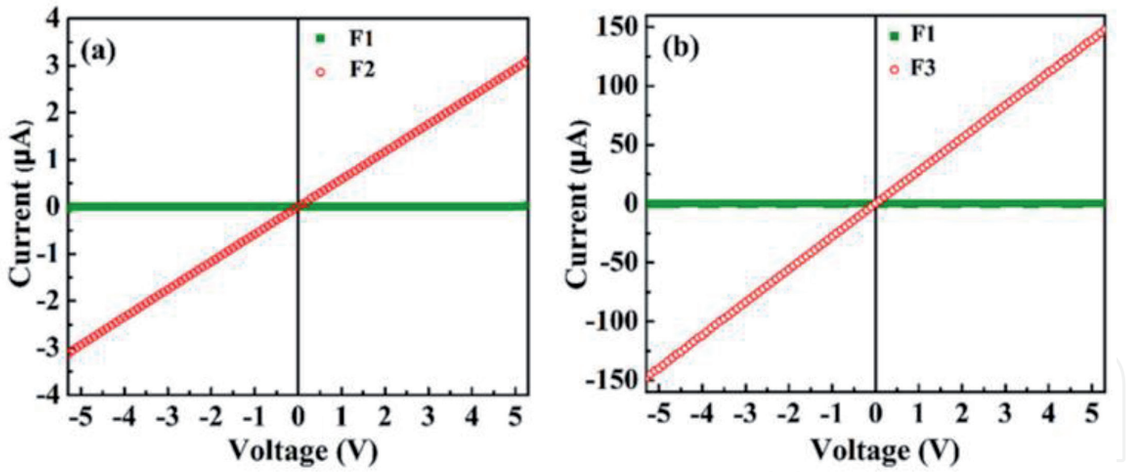

Figure 11.
I-V characteristics of (a) F2 in comparison to F1 and (b) F3 in comparison to F1. (Reprinted with permission from Bommidi et al. [8]).

enhance electrical conductivity significantly. As expected, the I–V characteristics (**Figure 11**) of F2 and F3 in comparison to F1 indicate a considerable increase in the electrical conductivity in them. At 5 V, the current values in F1, F2, and F3 are 4.4 nA, 3 μA, and 140 μA, respectively.

5. Conclusions

In this chapter, three unique surface modifications on a typical polycrystalline diamond thin film have been explained. The first modification has been direct patterning of deep sub-wavelength periodic features on the diamond thin film surface using linearly or circularly polarized fs-laser irradiation. It has also been shown that the surface features are perpendicular to the laser polarization. In other words, it has been demonstrated that laser polarization can be used to control the surface feature formation. The results discussed in Section 2 manifested that the interference of laser with surface plasmons is responsible for forming the surface features without any considerable changes in phase and crystallinity of the diamond thin film surface. Further studies should be taken up to control the shape and size of surface features by controlling different laser parameters such as energy, scan speed, polarization, etc. In Section 3, RTA was used to easily modify the top 100 nm of a polycrystalline diamond thin film surface into a surface with a considerable amount of sp^2 carbon, facilitating an excellent metal-free SERS activity as a consequence of the direct charge transfer resonance process. Moreover, RTA helped in fabricating an MIS-type structure with ease. SERS-based sensing study should be taken up to detect bio-molecules in real-time with an MIS-type biosensor. In Section 4, the N^+ ion beam was used to alter the sp^2 bonded carbon networks and incorporate N atoms into the surface and sub-surface regions in the typical polycrystalline diamond films. Consequently, the electrical conductivity of the diamond thin film was enhanced in several orders compared to the as-deposited film. By controlling the fluence of the ion beam, electrical conductivity can be controlled to a certain depth of the diamond thin film without considerable changes in the morphology and phase of diamond in the film. N^+ ion beam implantation also helped in fabricating an MIS-type structure with ease. Moreover, this method can be useful, especially when large-area diamond thin films have to be modified to make their surfaces electrically conductive.

DOI: http://dx.doi.org/10.5772/intechopen.98186

Author details

Vadali Venkata Satya Siva Srikanth
School of Engineering Sciences and Technology, University of Hyderabad, Hyderabad, India

*Address all correspondence to: vvsssse@uohyd.ac.in

References

[1] Vadali V S S S, Jiang X. Synthesis of diamond films. In: Brillas E, Martínez-Huitle C A, editors. Synthetic Diamond Films: Preparation, Electrochemistry, Characterization and Applications. Hoboken: John Wiley & Sons, Inc.; 2011. p. 21-55. DOI: 10.1002/9781118062364.ch2.

[2] Srikanth V V S S. Review of advances in diamond thin film synthesis. Proceedings of the Institution of Mechanical Engineers, Part C: Journal of Mechanical Engineering Science. 2011; 226:303-318. DOI: 10.1177/0954406211422788.

[3] Kratochvilova I. Polycrystalline diamond thin films for advanced applications. In: Silva AMT, Carabineiro SAC, editors. Advances in Carbon Nanostructures. London: IntechOpen; 2016. p. 161-173. DOI: 10.5772/64701.

[4] Brillas E, Martínez-Huitle C A, editors. Synthetic Diamond Films: Preparation, Electrochemistry, Characterization and Applications. Hoboken: John Wiley & Sons, Inc.; 2011. 632 p. DOI: 10.1002/9781118062364.

[5] Kuntumalla M K. Modification and enhanced Raman activity of nano-diamond and β-SiC thin film surfaces and Kelvin force microscopy and surface phonons of diamond/β-SiC nanocomposite thin films [thesis]. Hyderabad: University of Hyderabad; 2016.

[6] Kuntumalla M K, Rajamudili K, Desai N R, Srikanth V V S S. Polarization controlled deep sub-wavelength periodic features written by femtosecond laser on nanodiamond thin film surface. Applied Physics Letters. 2014; 104:161607. DOI: 10.1063/1.4873139.

[7] Kuntumalla M K, Srikanth V V S S, Ravulapalli S, Gangadharini U, Ojha H, Desai N R, Bansal C. SERS activity of Ag decorated nanodiamond and nano-β-SiC, diamond-like-carbon and thermally annealed diamond thin film surfaces. Physical Chemistry Chemical Physics. 2015; 17:21331-21336. DOI: 10.1039/c4cp05236f.

[8] Bommidi V. A study on uniquely modified diamond, diamond/β-SiC nanocomposite and graphene nitride (g-C_3N_4) surfaces [thesis]. Hyderabad: University of Hyderabad; 2019.

[9] Bommidi V, Kandasami A, Srikanth V V S S. N^+ ion beam irradiation as a strategy to enhance the electrical conductivity of polycrystalline diamond thin films. Materials Letters. 2019; 241:172-175. DOI: 10.1016/j.matlet.2019.01.085.